Materials Transactions, Vol. 44, No. 4 (2003) pp. 619 to 624
Special Issue on Platform Science and Technology for Advanced Magnesium Alloys, II

Precipitation in Mg–(4–13)%Li–(4–5)%Zn Ternary Alloys*1

Atsushi Yamamoto, Tetsuya Ashida*2, Yoshio Kouta*3, Kwang Bae Kim*4, Shinji Fukumoto and Harushige Tsubakino

Graduate School of Engineering, Himeji Institute of Technology, Himeji 671-2201, Japan

Precipitations in Mg–Li–Zn ternary alloys containing 4 to 13%Li and 4 to 5%Zn (in mass%) with α or β single phase, or with $(\alpha + \beta)$ dual phases were investigated using a micro-Vickers hardness measurement and transmission electron microscopy. Age hardening in the α phase alloy was found to occur, which was attributed to the precipitation of the stable θ (MgLiZn) phase with the following orientation relationships: $[10\bar{1}0]_\alpha \parallel [110]_\theta$, $(0001)_\alpha \parallel (1\bar{1}\bar{1})_\theta$. In the $(\alpha + \beta)$ phases alloy, the precipitation of the α phase together with the metastable θ' ($MgLi_2Zn$) phase occurred at grain boundaries between the α and β, and also β and β grains. The orientation relationships between the α and θ' were as follows; $(0001)_\alpha \parallel (01\bar{1})_{\theta'}$, $[0\bar{1}10]_\alpha \parallel [111]_{\theta'}$. Age hardening in the β alloy was caused by the precipitation of the θ' phase and over-aging was attributed to the precipitation of the α and θ phases.

(Received October 21, 2002; Accepted February 5, 2003)

Keywords: *Mg–Li–Zn alloy, precipitation, metastable phase, transmission electron microscopy (TEM), age hardening*

1. Introduction

Magnesium and its alloys have been recently used for portable electronic devices because of their advantages in lightness and recycleability. On the view point of lightness, Mg–Li alloys, with the lightest metallic element, lithium, have been investigated by many researchers.[1–3] In the Mg–Li alloy, bcc phase, β, is formed by Li addition of more than 6 mass%, which leads to improve the poor formability in magnesium alloys.[2] Additionally, superplastisity in the alloys contained third element was reported.[4] The authors also reported that the superplastic deformation occurred in the thermo-mechanically treated Mg–Li–Zn alloys.[5] Although the alloys are chemically active, semi-solidified state is capable for forming.[6] The alloys with Mg–Li system have superior properties in the view point of lightness and formability. On the other hand, Mg–Li alloys have a disadvantage in mechanical property, that is, yield strength and tensile strength are too low for engineering usages. Although the relationships between heat treatment and mechanical properties were reported,[7–10] precipitation phenomena were not investigated in detail. It is considered to be due to the difficulty for preparing foil specimens for electron transmission microscopy (TEM). The authors carried out TEM observations on β phase Mg–Li–Zn alloys, and reported precipitation sequence and orientation relationships between precipitates and the matrix, in the previous study.[10]

In the present study, precipitation phenomena in Mg–Li–Zn alloys with α (hcp) phase, $(\alpha + \beta)$ phase and β phase are reported.

2. Experimental Procedures

The alloys were prepared by the same procedures reported in the previous paper,[10] that is, magnesium and lithium with 3N grade, and zinc with 4N grade were melted with compositions of 4–13 and 4–5 mass% for lithium and zinc, respectively, in a high frequency electric furnace under an argon atmosphere. Chemical compositions of the alloys are listed in Table 1. The compositions of the alloys are shown in Fig. 1 which was the Mg–Li–Zn ternary phase diagram reported by Weinberg *et al.*[11]

Table 1 Chemical compositions of alloys (mass%).

	Li	Zn
α phase alloy	4.4	4.3
$(\alpha + \beta)$ phases alloy	8.2	4.6
β phase alloy	13.2	4.8

The specimens were solution heat-treated at 723 K for 3.6 ks in an argon atmosphere and then quenched into ice water. Microstructures of Mg–4.4Li–4.3Zn, Mg–8.2Li–4.6Zn and Mg–13.2Li–4.8Zn (mass%) alloys in as quenched condition showed α single phase, $(\alpha + \beta)$ dual phase and β single phase, respectively, so these alloys are named as α, $(\alpha + \beta)$ and β alloys, respectively. After quenching, the specimens were aged at the temperatures of R. T. to 523 K. Foils for TEM observations were chemically polished using a nitric acid : methanol : glycerin = 1 : 1 : 1 solution, electropolished at R. T. using a phosphoric acid : ethanol = 3 : 5 solution, and then finished by a twin-jet method at R. T. using the same solution as the electropolishing.

3. Results and Discussion

3.1 α phase alloy

Changes in hardness in the α phase alloy at various temperatures are shown in Fig. 2. Age hardening and over-age softening were observed at aging temperatures ranging 383 to 523 K, while peak hardening was not accomplished at the temperatures between R. T. and 348 K for the aging time up to 10^4 ks. Although there were few reports on precipitation in α phase alloys, Matsuzawa *et al.*[12] reported that age hardening was not detected in Mg–4.7Li–0.9Al (mass%) (−0.72 at%Al) alloy aged at temperatures between R. T. to

*1This Paper was Originally Published in J. J. I. L. M **51** (2001), 604–607.
*2Graduate Student, Himeji Institute of Technology. Present address: Mitsubishi Cable Industries, LTD. Amagasaki, 660-0856, Japan.
*3Graduate Student, Himeji Institute of Technology. Present address: Kobe University, Kobe 657-8501, Japan.
*4Hankuk Aviation University (Korea).

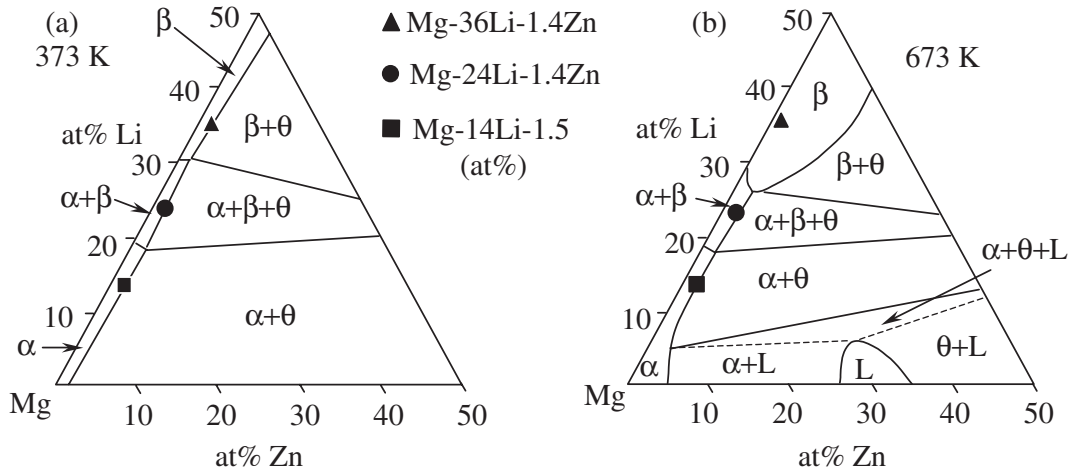

Fig. 1 Compositions of the alloys shown in Mg corner in Mg–Li–Zn ternary alloy phase diagram.[11] Isothermal cross sections at (a) 373 and (b) 673 K.

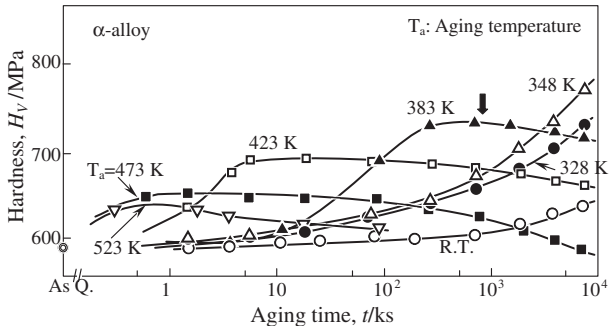

Fig. 2 Change in hardness during aging at various temperatures in the α phase alloy (Mg–4.4Li–4.3Zn alloy). The bold arrow indicates the aging condition for TEM observations.

423 K. Higher concentration of zinc in the alloy used in the present study, about 4 mass% (1.5 at%), seems to cause the age hardening in the α phase alloy.

Microstructures in the specimen aged at 383 K for 860 ks, peak aging condition indicated by the bold arrow in Fig. 2, were observed by TEM and shown in Fig. 3. Plate-like precipitates were formed as shown in the bright field image (BFI), Fig. 3(a). The selected area diffraction pattern (SADP), Fig. 3(c), was taken under the condition of $\vec{B} \parallel [10\bar{1}0]_\alpha$ where $\vec{B}$ is the incident beam direction. Extra spots due to precipitates and double diffraction, and streaks perpendicular to the longitudinal axis of the precipitates appear in Fig. 3(c). As shown in the key diagram in Fig. 3(d), the SADP is indexed as that of the matrix α phase (hcp; $a_0 = 0.319$, $c_0 = 0.514$ nm[13]) and the stable phase precipitate θ (MgLiZn, cubic; $a_0 = 0.744$ nm[3]). The dark field image (DFI), Fig. 3(b), was taken with $1\bar{1}1_\theta$ spot. The key diagram, Fig. 3(d), shows the orientation relationships between the θ and the matrix α are as follows: $[10\bar{1}0]_\alpha \parallel [110]_\theta$ and $(0001)_\alpha \parallel (1\bar{1}\bar{1})_\theta$. In the previous paper,[10] orientation relationships between β and α, and β and θ were reported as follows: $(011)_\beta \parallel (0001)_\alpha$, $[1\bar{1}1]_\beta \parallel [2\bar{1}\bar{1}0]_\alpha$ and $(\bar{1}11)_\beta \parallel (\bar{1}12)_\theta$, $[110]_\beta \parallel [1\bar{1}1]_\theta$, respectively, which leads to the following orientation relationships: $\{011\}_\beta \parallel \{0001\}_\alpha \parallel \{111\}_\theta$ and $\{111\}_\beta \parallel \{2\bar{1}\bar{1}0\}_\alpha \parallel \{112\}_\theta$. Therefore, the orientation relationships between α and θ are deduced as $(0001)_\alpha \parallel (1\bar{1}\bar{1})_\theta$ and $[2\bar{1}\bar{1}0]_\alpha \parallel [211]_\theta$. The latter is equivalent to $[10\bar{1}0]_\alpha \parallel [110]_\theta$. The orientation relationships between α and θ obtained in the present study are consistent with the previous results. However, since the α and θ phases were independently formed in the matrix β,[10] the same orientation relationships do not mean any necessity but imply that the close-packed plane of the θ phase is formed on the close-packed plane of α matrix. The precipitates in Fig. 3(a) were formed on the $(0001)_\alpha$ plane which is parallel to $(1\bar{1}\bar{1})_\theta$ plane. Spacings of these planes are 0.512 and 0.430 nm, respectively. When they are multiplied by a factor of 4 and 5, respectively, the spacings of 2.06 and 2.15 nm were obtained. The spacing of $(1\bar{1}\bar{1})_\theta$, 2.15 nm, is larger than that of $(0001)_\alpha$. The strain contrasts around the precipitates in Fig. 3(a) are due to the difference in the lattice spacings, which leads to age hardening.

3.2 ($\alpha + \beta$) dual phase alloy

Microstructures in the ($\alpha + \beta$) dual phase alloy are shown in Fig. 4. In the specimens quenched from 723 K, Fig. 4(a), bright grains and dark grains are observed, which correspond to α and β phase grains, respectively. Plate like contrasts in the α grains are due to twins induced by emery polishing. Microstructures observed in the specimen aged at 473 K for 245 ks are shown in Fig. 4(b). Precipitation of α phase grains was observed at α/β grain boundaries and β/β boundaries, which are indicated in Fig. 4(b) by the arrows A and B, respectively.

Changes in hardness in ($\alpha + \beta$) phases alloy are shown in Fig. 5. Since the alloy was composed of α and β grains in as quenched condition as shown in Fig. 4, hardness changes in those phase grains were separately measured. Changes in hardness in the β grain are shown for each temperature. However, hardness in the α grain did not show any changes at any aging conditions, so the hardness change in α grain at 423 K was shown in this figure. Peak hardness in the β grain was observed at R. T. and 328 K, while softening occurred at temperatures of 348, 383 and 423 K. Age hardening in the β phase alloy is attributed to precipitation of metastable θ' phase, while the precipitation of the stable α and θ phases

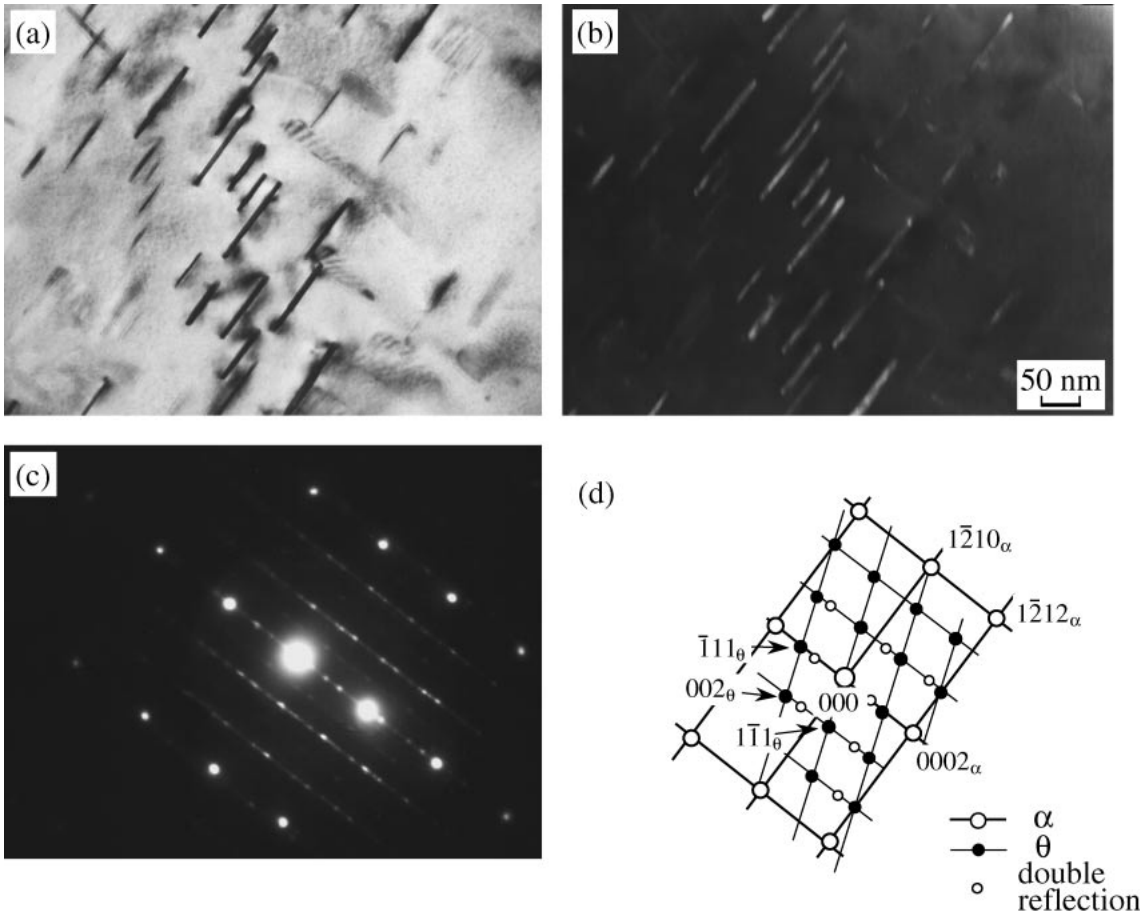

Fig. 3 TEM observations of the α phase alloy (Mg–4.4Li–4.3Zn alloy) aged at 383 K for 860 ks. (a) BFI, (b) DFI taken with $1\bar{1}1_\theta$ spot, (c) SADP and (d) key diagram for the SADP.

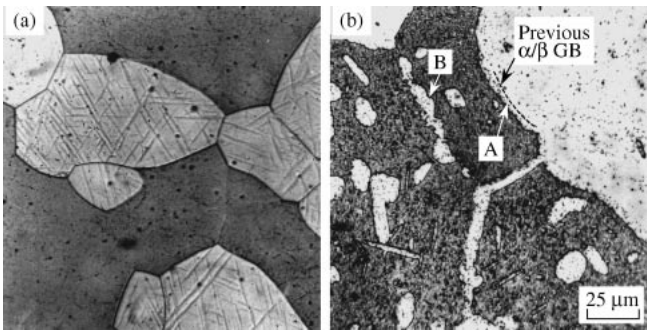

Fig. 4 Microstructures in ($\alpha + \beta$) phases alloy (Mg–8.2Li–4.6Zn alloy). (a) As quenched and (b) aged at 473 K for 245 ks.

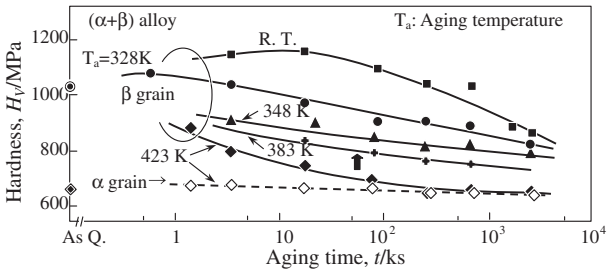

Fig. 5 Change in hardness during aging at various temperatures in an ($\alpha + \beta$) phases alloy (Mg–8.2Li–4.6Zn alloy). The bold arrow indicates the aging condition for TEM observations.

results in softening.[10] In the present ($\alpha + \beta$) phases alloy, it is considered that hardening occurred at the early stage of aging, faster than the shortest measuring period in this study, which was followed by precipitation of the stable phases to be decreased in hardness. The specimen aged at 383 K for 58 ks, indicated by the bold arrow in Fig. 5, was observed by TEM, the results of which are shown in Fig. 6.

Microstructures near a grain boundary between α and β grains are shown in Fig. 6(a), in which the upper and lower portions are α and β grains, respectively. The α grain developed into the β grain during aging. The dark field micrograph, Fig. 6(b), taken with the α spot shows that the newly developed α grain has the same orientation as the original α grain. Precipitates are observed in the β grain and newly developed α grain. Figure 7 shows selected area diffraction patterns taken in the α, developed α and β regions, (a), (b) and (c), respectively. Incident beam directions, $\vec{B}$, in Figs. 7(a) and (b) are parallel to $[0001]_\alpha$, while that in Fig. 7(c) is parallel to $[1\bar{1}1]_\beta$. There are no extra spots in Fig. 7(a). The SADP, Fig. 7(c), can be indexed as the β phase (bcc: $a_0 = 0.325$ nm[13]), α phase and variants of α. The orientation relationships between α and β are $(111)_\beta \parallel (1\bar{2}10)_\alpha$, $(\bar{1}01)_\beta \parallel (0001)_\alpha$. This orientation relationships are the same as those between the β matrix and α precipitates in the Mg–11Li–10Zn (mass%) alloy as reported in the previous paper.[10] The SADP shown in Fig. 7(b) is complex, but it can be analyzed as due to α matrix, metastable precipitates θ'

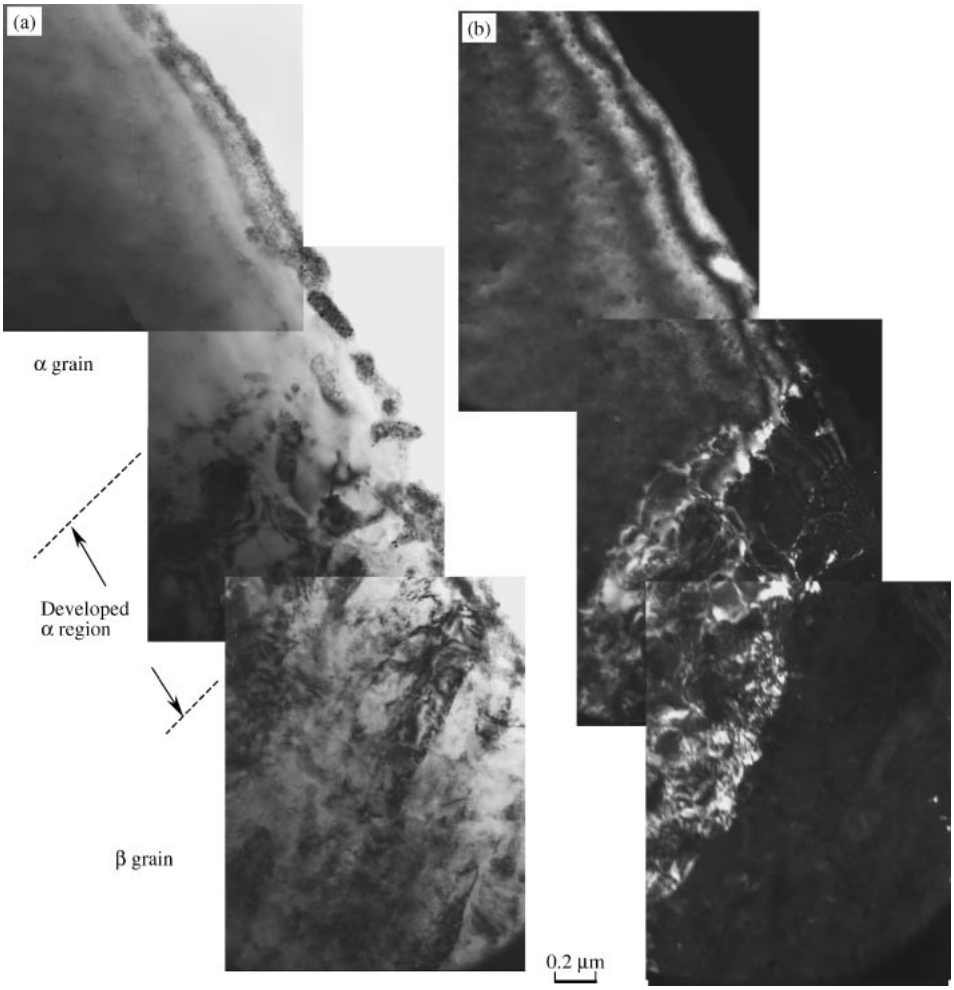

Fig. 6 TEM images of the ($\alpha + \beta$) phases alloy (Mg–8.2Li–4.6Zn alloy) aged at 383 K for 58 ks. (a) BFI and (b) DFI taken with an α spot.

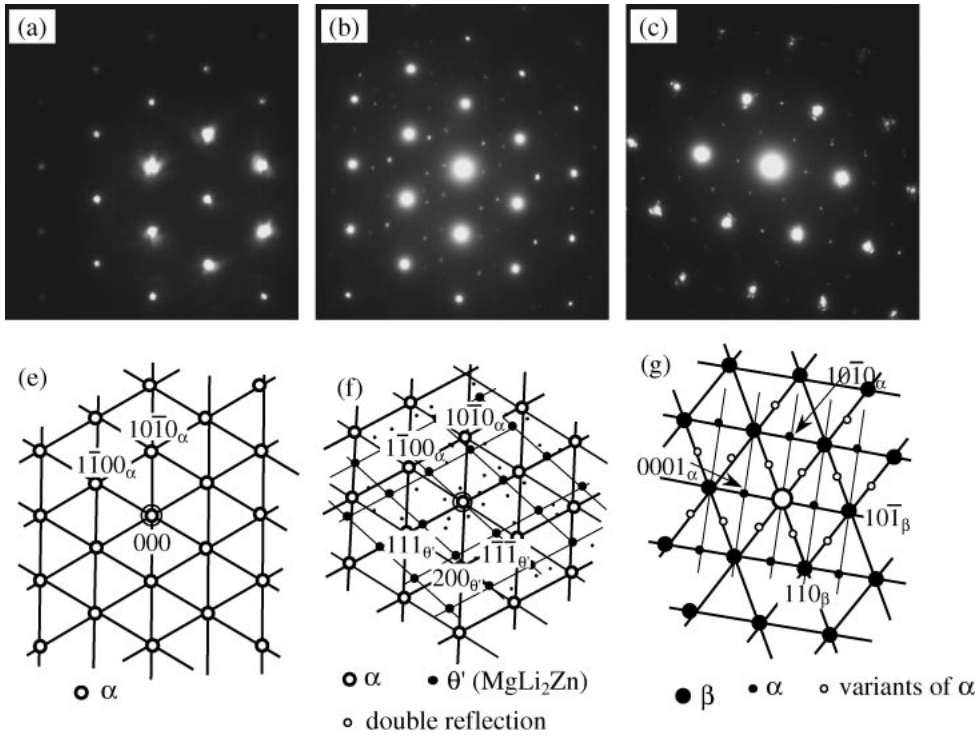

Fig. 7 Selected area diffraction patterns taken at α grain (a), precipitated α grain (b) and β grain (c) shown in Fig. 6. Key diagrams (e), (f) and (g) are for (a), (b) and (c), respectively.

($MgLi_2Zn$: fcc, $a_0 = 0.664\,nm$[14]) and double reflections of θ' due to α matrix. It is considered that supersaturated β did not decompose into α and θ, but into α and θ' which has a higher Li concentration than that in θ. The orientation relationships between α and θ' are $(0001)_\alpha \parallel (01\bar{1})_{\theta'}$, $[0\bar{1}10]_\alpha \parallel [111]_{\theta'}$. It is well known that the metastable θ' precipitates are formed in β alloys, but stable θ precipitates are formed in α alloys as mentioned in 3.1, therefore the orientation relationships between α and θ' have been reported for the first time by the present study.

3.3 β phase alloy

As mentioned above, there is the previous paper reported about precipitation in a β phase alloy (Mg–11Li–10Zn).[10] The β phase alloy used in this study has higher Li and lower Zn concentrations compared with the previous alloy. Changes in hardness are shown in Fig. 8. Hardness increased and then decreased through peak hardening at all the aging temperatures, while in the previous alloy, softening occurred at higher aging temperatures.[10] Precipitation of θ phase is considered to be delayed due to low Zn concentration in the present alloy. Microstructural observations by TEM on the specimens aged at the conditions indicated by the bold arrows a and b in Fig. 8, 328 K, 1.7 Ms and 473 K, 83 ks, were shown

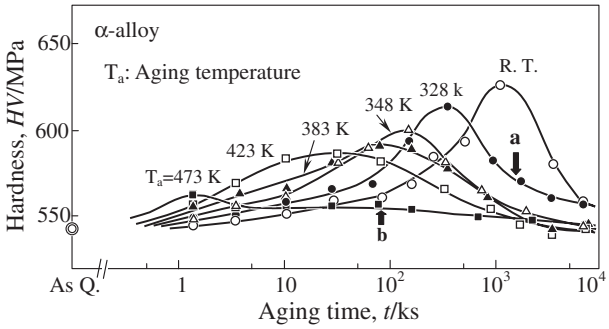

Fig. 8 Change in hardness during aging at various temperatures in the β phase alloy (Mg–13.2Li–4.8Zn alloy). The bold arrows indicate the aging condition for TEM observations.

in Figs. 9 and 10, respectively. In briefly, θ' and α precipitates were formed in the specimens aged at 328 K for 1.7 Ms, while θ precipitates were formed by aging at 473 K for 83 ks. Orientation relationships between β-θ', β-α and β-θ are as follows, respectively: $(011)_\beta \parallel (011)_{\theta'}$, $[100]_\beta \parallel [100]_{\theta'}$, $(011)_\beta \parallel (0001)_\alpha$, $[1\bar{1}1]_\beta \parallel [2\bar{1}\bar{1}0]_\alpha$ and $(\bar{1}11)_\beta \parallel (\bar{1}12)_\theta$, $[110]_\beta \parallel [1\bar{1}1]_\theta$. In the over aged condition, Fig. 10, α phase was not observed, which is believed to be due to the higher Li concentration in the present alloy than

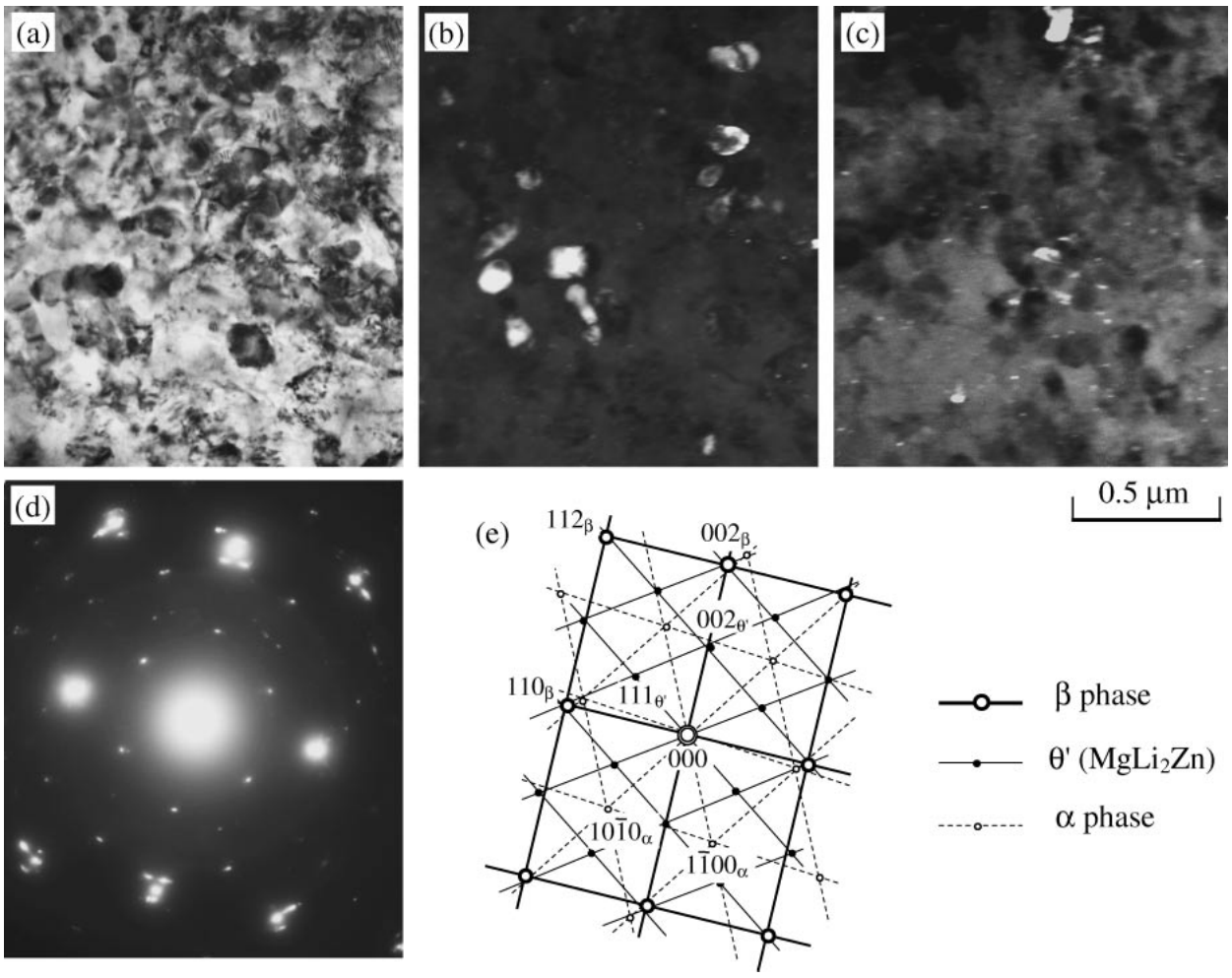

Fig. 9 TEM observations in the β phase alloy (Mg–13.2Li–4.8Zn alloy) aged at 328 K for 1.7 Ms. (a) BFI, (b) DFI taken with $111_{\theta'}$ spot, (c) DFI taken with $1\bar{1}00_\alpha$ spot, (d) SADP and (e) key diagram for the SADP.

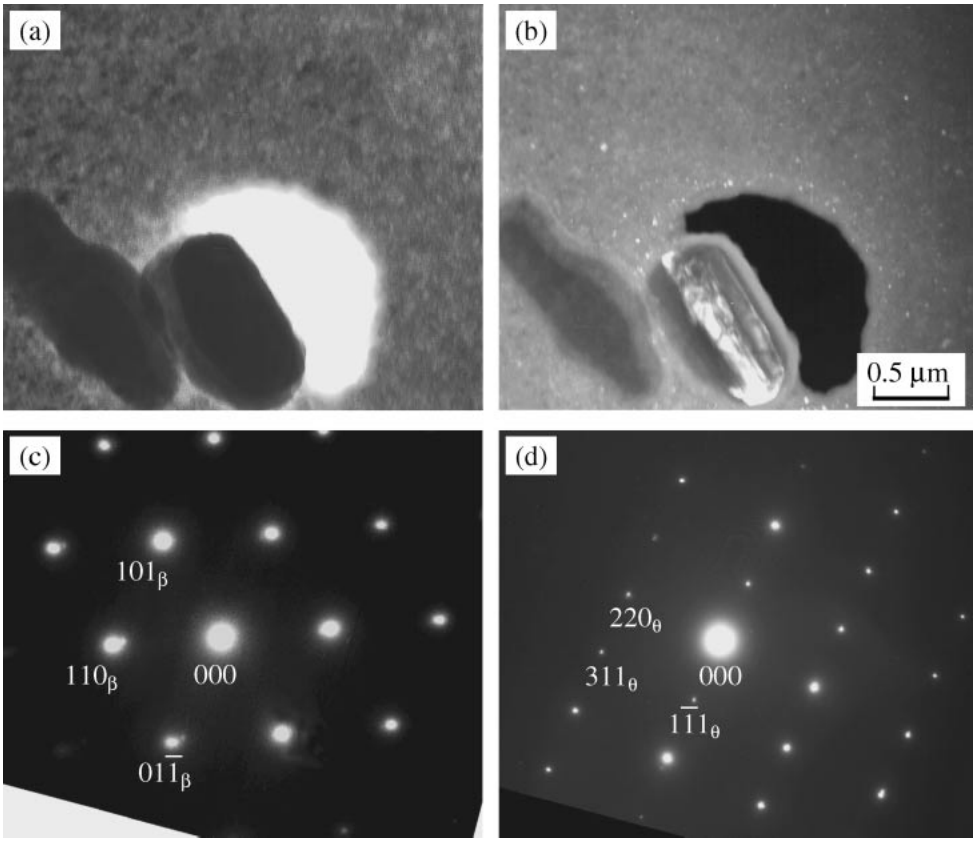

Fig. 10 TEM observation of the β phase alloy (Mg–13.2Li–4.8Zn alloy) aged at 473 K for 83 ks. (a) BFI, (b) DFI taken with 111_θ spot, (c) SADP for the β matrix and (d) SADP for the precipitate.

the previous one. That is, the Li and Zn concentrations in the previous alloy were about 30.3 and 3.3 at%, respectively, the composition of which is positioned on $(\beta+\theta)/(\alpha+\beta+\theta)$ boundary (see Fig. 1(a)), while the compositions of the present β alloy is far from the boundary.

4. Summary

Precipitations in ternary magnesium alloys contained Li and Zn in the range of 4–13 and 4–5 mass%, respectively, were investigated and the following results were obtained.

(1) According to TEM observations, the hardening is attributed to the precipitation of θ phase in the α phase alloy. Orientation relationships between α and θ are as follows: $[10\bar{1}0]_\alpha \parallel [110]_\theta$, $(0001)_\alpha \parallel (1\bar{1}\bar{1})_\theta$.

(2) Precipitation in β grains in $(\alpha+\beta)$ phases alloy is the same as that in a β single phase alloy. Precipitation of α phase was observed at α/β and β/β grain boundaries. In such precipitated α grains θ' precipitates were formed. The orientation relationship between α and θ' are as follows: $(0001)_\alpha \parallel (01\bar{1})_{\theta'}$, $[0\bar{1}10]_\alpha \parallel [111]_{\theta'}$.

(3) Age hardening and softening in β phase alloy are induced by precipitation of the metastable θ' phase, and stable α and θ phases, respectively.

REFERENCES

1) J. H. Jackson, P. D. Frost, A. C. Loonam, L. W. Eastwood and C. H. Lorig: Trans. AIME. **185** (1949) 149–168.
2) W. R. D. Jones: J. Inst. Metals **84** (1955–56) 364–378.
3) W. R. D. Jones and G. V. Hogg: J. Inst. Metals **85** (1956–57) 255–261.
4) Y. Kojima, M. Inoue and A. Tanno: J. Japan Inst. Metals **54** (1990) 354–355.
5) A. Yamamoto, Y. Kouta and H. Tsubakino: *Proc. 4th Inter. Conf. on Recrystallization and Related Phenomena*, ed. T. Sakai and H. G. Suzuki, (The Japan Inst. Metals 1999) 833–838.
6) R. Chandran, T. Sakai, S. Kamado and Y. Kojima: J. JILM **48** (1998) 13–18.
7) K. Matsuzawa, T. Koshihara, S. Ochiai and Y. Kojima: J. JILM **40** (1999) 659–665.
8) H. Hatta, Z. Li, S. Kamado and Y. Kojima: J. JILM **45** (1995) 702–707.
9) H. Hatta, R. Chandran, S. Kamado and Y. Kojima: J. JILM **47** (1997) 195–201.
10) A. Yamamoto, T. Ashida and H. Tsubakino: J. JILM **42** (1992) 797–803.
11) A. F. Weinberg, D. W. Levinson and W. Rostoker: Trans. ASM **48** (1956) 855–871.
12) K. Matsuzawa, T. Koshihara and Y. Kojima: J. JILM **39** (1989) 45–51.
13) F. H. Herbstein and B. L. Averbach: Acta Metall. **4** (1956) 407–413.
14) J. B. Clark and L. Sturkey: J. Inst. Metals **86** (1957–58) 272–276.